The stereochemistry of a four-way DNA junction: a theoretical study

Eberhard von Kitzing, David M.J.Lilley[1] and Stephan Diekmann[2]
Abteilung Zellphysiologie, Max-Planck-Institut für Medizinische Forschung, Postfach 103820, D-6900 Heidelberg, FRG,[1] Department of Biochemistry, The University, Dundee DD1 4HN, UK and [2]Abteilung Molekulare Biologie, Max-Planck-Institut für Biophysikalische Chemie, Am Fassburg, D-3400 Göttingen-Nikolausberg, FRG

Received January 19, 1990, Revised and Accepted March 7, 1990

ABSTRACT

The stereochemical conformation of the four-way helical junction in DNA (the Holliday junction; the postulated central intermediate of genetic recombination) has been analysed, using molecular mechanical computer modelling. A version of the AMBER program package was employed, that had been modified to include the influence of counterions and a global optimisation procedure. Starting from an extended planar structure, the conformation was varied in order to minimise the energy, and we discuss three structures obtained by this procedure. One structure is closely related to a square-planar cross, in which there is no stacking interaction between the four double helical stems. This structure is probably closely similar to that observed experimentally in the absence of cations. The remaining two structures are based on related, yet distinct, conformations, in which there is pairwise coaxial stacking of neighbouring stems. In these structures, the four DNA stems adopt the form of two quasi-continuous helices, in which base stacking is very similar to that found in standard B-DNA geometry. The two stacked helices so formed are not aligned parallel to each other, but subtend an angle of approximately 60°. The strands that exchange between one stacked helix and the other are disposed about the smaller angle of the cross (i.e. 60° rather than 120°), generating an approximately antiparallel alignment of DNA sequences. This structure is precisely the stacked X-structure proposed on the basis of experimental data. The calculations indicate distortions from standard B-DNA conformation that are required to adopt the stacked X-structure; a widening of the minor groove at the junction, and reorientation of the central phosphate groups of the exchanging strands. An important feature of the stacked X-structure is that it presents two structurally distinct sides. These may be recognised differently by enzymes, providing a rationalisation for the points of cleavage by Holliday resolvases.

INTRODUCTION

Helical junctions are an important component of a number of biologically important nucleic acids. Many structured RNA molecules, typified by tRNA, exhibit interaction between double helical segments, including molecules that are very important in transcript splicing. Such structures also occur in DNA molecules and are particularly significant in intermediates involved in DNA rearrangements like recombination.

Homologous genetic recombination may occur between DNA molecules containing extensive regions of close homology, and creates genome diversity by the exchange of genetic markers. The four-way DNA junction (or Holliday intermediate; 1–6) is believed to be the central intermediate in homologous recombination as well as certain kinds of site-specific recombination events (7–10). One of the most critical stages of recombination is the resolution process, where unconnected duplexes are regenerated. This is brought about by resolvase enzymes that must recognise the structure of the junction and cleave it. Cleavage can occur in one of two ways, generating different recombination products, and thus the nature of the interaction will determine the outcome of the recombination process. However, despite the importance of these intermediates, their structure has been poorly understood until recent times, to the detriment of our understanding of the structural basis of recombination. We are unlikely to understand the details of the resolution process without a detailed knowledge of the structure of the junction itself.

Four-way junctions have been visualised by electron microscopy, but recent experimental progress in understanding the structure of these species has been based on the ability to construct DNA junctions *in vitro*, using synthesised (11,12) or cloned (13) oligonucleotides. In early experiments based on gel electrophoretic mobility we demonstrated that the inclusion of a four-way junction into a DNA fragment was equivalent to forming a sharp bend or kink at that position (13), and we later showed that the binding of metal ions alters the conformation of such junctions and increase their thermal stability (14). The first clue as to the three-dimensional shape of the junction came from the work of Cooper and Hagerman (15) who studied the

* To whom correspondence should be addressed

relative electrophoretic mobilities of a small synthetic junction to which reporter arms had been ligated in various combinations. They concluded that the shape could not be tetrahedral, and deduced an asymmetric configuration of the four helical arms.

Using a related technique, we studied the configuration of a series of junctions constructed from eighty base oligonucleotides. As a result we proposed a general model for the helical junction, termed the stacked X-structure (16). The essential details of the model were subsequently confirmed using fluorescence energy transfer spectroscopy (17). The main features of the proposed structure are:

1. The overall shape of the junction is that of an X, where quasi-continuous helices are derived by pairwise stacking of the helical arms. These then rotate (in the manner of opening a pair of scissors) to avoid clashes and electrostatic repulsion. The symmetry of the structure is also consistent with the results of hydroxyl radical probing of small synthetic junctions (14) and experiments of Cooper and Hagerman (15). The concept of helix-helix stacking was incorporated in a model of the Holliday junction built by Sigal and Alberts (19), and is to some extent analogous to the stacking of the T and acceptor arms in tRNA.

2. The choice of stacking partners is governed by the sequence at the junction. Two isomeric structures are possible in principle for any sequence depending on whether a given helical arm stacks with its neighbour to its left or right. We found that for our sequences the junctions adopted one predominant isomeric conformation only, but which isomer was observed depended on the local sequence at the junction.

3. The pattern of cleavage of junctions by phage resolvases, such as T4 endonuclease VII, depends on the isomeric form adopted for a given DNA sequence. Mueller *et al* (20) also noted that resolvase cleavage of junctions depends on the local sequence.

4. In the absence of metal ions the structure is radically different. Without salt the junctions of any sequence appear to adopt a structure close to square-planar in which the four arms are unstacked and maximally extended (16).

In this paper we present the structure of a four-way DNA junction obtained by energy minimisation studies. The sequence chosen (see Figure 1) possesses the same central sequence as a junction we have studied experimentally (16,17). It comprises six base pairs in each helical stem. The energy of several structural isomers were minimised, and that with the lowest energy has properties in good agreement with the experimental data.

THEORETICAL METHODS

We applied theoretical methods to obtain the three-dimensional structure of a DNA four-way junction. Molecular model building techniques were employed, followed by global and local structure optimisation. Finally we explain how the structure obtained was analysed.

Generating four-way junctions

A modified version of the AMBER program package (21,22) was used for molecular mechanics calculations. A Debye-Hückel type potential for every single charge was introduced to account for averaged electrostatic interactions of the counter-ions (23,24). In addition, an improved optimisation procedure was employed (23,25).

For standard A-DNA or B-DNA structures, published coordinates may normally be taken as reasonably good starting structures. However, this approach cannot be used for calculating DNA four-way junctions, since these differ radically from simple double helical DNA. The starting structures had to be generated *ab initio*.

An extended four-way junction (the precursor of structures discussed in the Results section) was generated by means of an interactive program to serve as the starting structure for the optimisation. The sequence at the junction (the first two base pairs of each stem) of the optimised structure was chosen to be identical to that of junction 1 that was extensively studied experimentally (16,17). The sequence was generated by taking the innermost two base pairs on each arm from this junction 1, and repeating them twice. The resulting junction contains six base pairs in each helical stem. The full sequence is displayed in Figure 1.

Optimisation

In molecular mechanics calculation, the structure of a given molecule is modified in order to minimise the structural energy. Due to local convergence of standard optimisation procedures, these calculations often yield a structure with a relatively low energy in the close vicinity of the starting structure, and in general the structure with the absolutely lowest structural energy (the global minimum) is not found. In the program package used here, special optimisation routines were introduced to reduce this problem of local minima.

Any type of global optimisation requires an exhaustive search for various possible structures. Because the number of required calculations grows exponentially with the number of degrees of freedom, a global optimisation for our four-way junction structure taking into account all atoms ($\sim$1100 atoms, resulting in 3300 degrees of freedom) is far beyond our available computer time. Therefore, we selected only very few degrees of freedom for the global optimisation. As described below, only rotations around certain pairs of distant atoms are introduced to change the global conformation of the junction. Another application of this principle of drastically reducing the variable space has been given by Sklenar *et al* (26).

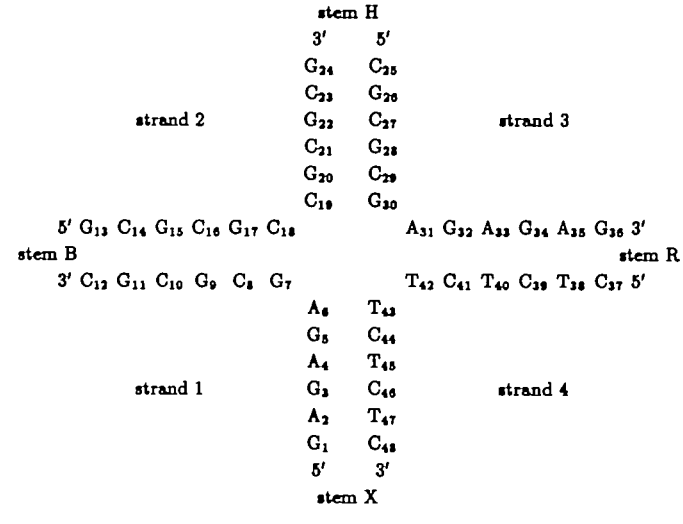

Figure 1. The DNA sequence of the optimised structures. The sequence is closely related to that of junction 1 used in experimental studies of the four-way junction (16) The first two bases in each stem at the junction are identical with the experimental sequence

For global optimisation the Bremermann method (27,28) was applied, which has been shown to be reasonably successful (29). At the beginning of the optimisation, a starting point has to be given, and its energy must be calculated. Then, the method works in an iterative manner. The starting point and its structural energy for a certain cycle is taken from the previous cycle. For n variables n random numbers are generated obeying a Gaussian distribution These numbers represent a random direction in the space of the variables. Four additional points are generated along this direction in the neighbourhood of the actual values of the variables. The structural energies of these points are calculated. A fourth order polynomial is determined to interpolate these four new energies together with the energy of the starting structure. This polynomial describes the variation of the energy along the chosen line in the parameter space. The global minimum of this one dimensional interpolation is calculated by means of the Cardan formula. The structural energy of the DNA conformation corresponding to this minimum is determined, and the energies of the starting structure, the four additional structures, and the expected global minimum structure are compared. The structure with the lowest energy serves as the starting point for the next optimisation cycle.

Only 12 to 36 rotational angles (see below) were used as variables in this global optimisation procedure. The remaining degrees of freedom of the 1100 atoms were relaxed towards a minimum for the structural energy at every step by means of a local conjugated gradient optimisation (25) of the structure. Thus the slow global Bremermann optimisation with random direction search is used only for a very small subspace, whereas the fast locally converging method of conjugated gradients is used for all degrees of freedom. In our application of the Bremermann optimisation method, a calculation of the structural energy means the variation of a fixed small number of variables, followed by a local optimisation using the method of conjugated gradients, binding the atoms to the actual starting position by a harmonic force of 10 kcal/(Mol Å^2). This allows the relaxation of distorted bond angles and close atomic contacts. The energy which results from this local optimisation with initial constraints, is taken as the structural energy in the Bremermann optimisation. Further details will be given by Kitzing and Diekmann (in preparation).

The structures created during the optimisation process were generated by rotations around the axes connecting pairs of oxygen atoms at the four-way junction that are illustrated in Figure 2. Twelve rotational axes have been introduced; these are:

1. $O_{5'B}-O_{3'B}$	2 $O_{5'H}-O_{3'H}$	3. $O_{5'R}-O_{3'R}$	4. $O_{5'X}-O_{3'X}$
5. $O_{3'B}-O_{5'H}$	6. $O_{3'H}-O_{5'R}$	7. $O_{3'R}-O_{5'X}$	8 $O_{3'X}-O_{5'B}$
9. $O_{5'B}-O_{5'R}$	10. $O_{3'B}-O_{3'R}$	11. $O_{5'H}-O_{5'X}$	12. $O_{3'H}-O_{3'X}$

Rotation angles around these axes were used as the variables for the global Bremerman optimisation. Because these rotations do not commute, some axes were used up to three times (12 rotational angles used up to three times results in maximally 36 angles).

Analysis of the four-way junction structure

The structure of the four-way junction was analysed according to the helical parameter definitions suggested at the EMBO workshop on DNA Curvature and Bending (30). In addition to the local conformation of the junctions, the mutual orientations of the axes of each of the four DNA stems are of particular interest. Therefore, the average helix axes z_B, z_H, z_R and z_X of each stem were calculated. To determine the angles in space between these axes, we used the axes of inertia. The second moments of these axes are used to define an average axis z_g for all the four stems. The best plane for these axes is defined by the respective normal vector x_g. The orientation of the stem-axes are given as the angles ψ_N of the stem axes z_N to the global axis

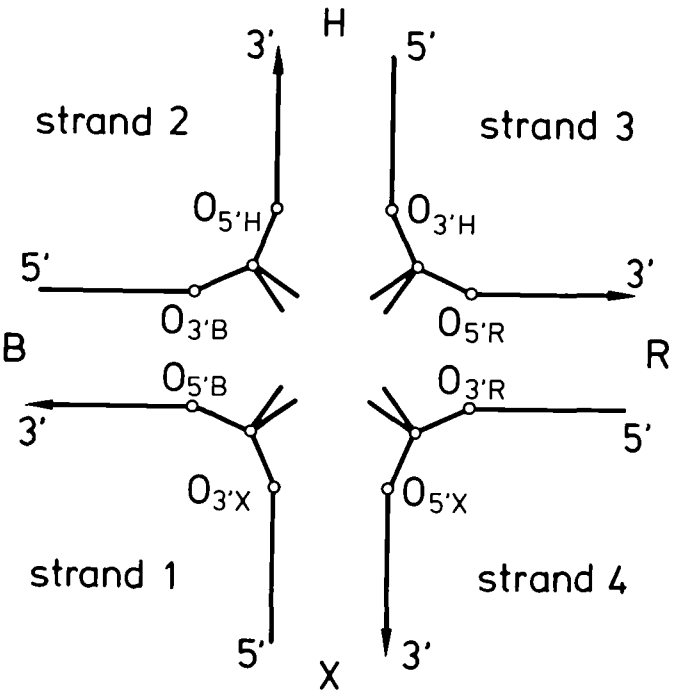

Figure 2. A schematic form of the four-way junction. It consists of the four arms B, H, R, and X, named from the restriction sites present in the arms of the experimentally analysed molecules (16) (*Bam*HI, *Hin*dIII, *Eco*RI and *Xba*I) The final structures were obtained by repeated rotations around the twelve axes (see text).

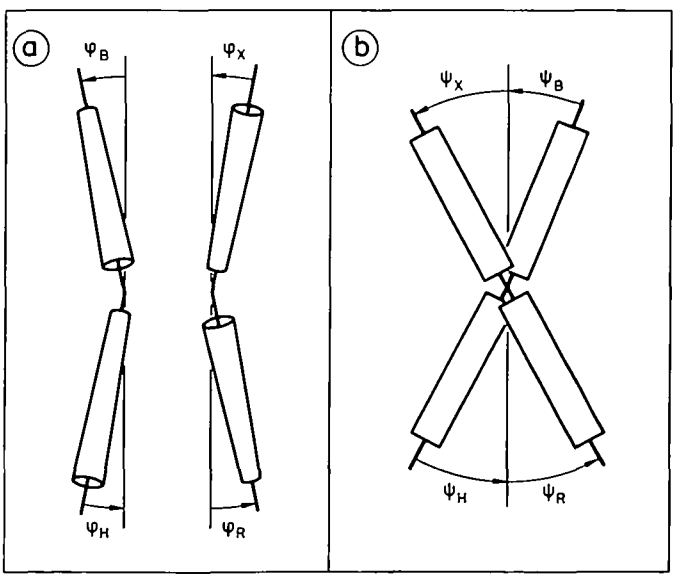

Figure 3. The angles of the four DNA helix stems with respect to their best plane. The best plane is defined by the four stem axes. a shows the out-of-plane angles ϕ_B, ϕ_X, ϕ_R and ϕ_H between the stems and the best plane In b ψ_B, ψ_X, ψ_R and ψ_H are the angles between the stem axes and the average axis projected on the best plane

z_g projected on the best plane with N being B, H, R or X (Figure 3b). The out-of-plane angle ψ_N is the angle between the stem axis z_N and the best plane (Figure 3a).

Coordinates of the optimised structures will be available on request, via BITNET: EKITSIN@DGOGWDG1.

RESULTS

A model of a DNA four-way junction was constructed containing an open centre with unstacked bases shown schematically in Figure 2. This extended structure was varied to obtain various starting structures for the global optimisation. Eight different structural isomers of this DNA molecule were obtained. All the structures fall into three distinct classes or intermediates between these classes. We will therefore only present structural details for three of these structures as representatives for each class. These comprise two isomers exhibiting helix-helix stacking (H_1 and H_2), and a third structure with an open unstacked conformation (E).

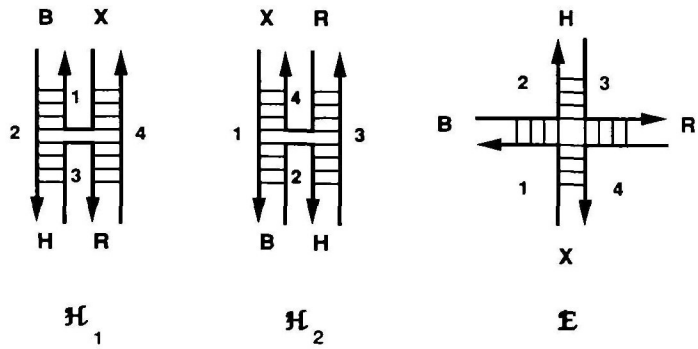

Figure 4. Three distinct structures were obtained by the optimisation, and are displayed in a schematic form. Two of them have a form close to an 'H' and are therefore designated as H_1 and H_2. They consist of two pairs of coaxially stacked helical stems. These two isomeric forms H_1 and H_2 differ in which stem stacks on which of the two neighbouring partners. The third variant has an extended structure which is designated by E. The 5′ to 3′ direction is indicated by the arrows.

Because of the large number of local energy minima, a given minimum cannot positively be identified as the global minimum having the absolutely lowest energy. Furthermore, molecules in solution will thermally populate a large number of structures. As a consequence, the global minimum structure may deviate considerably from the average of the populated structures. We will therefore concentrate on those properties of the calculated four-way junctions that we consider to be of more general importance, and discuss only those atomic details of the structures that seem to be independent of the particular properties of a given local minimum. We will first present the general geometry of the junction and then discuss the atomic details.

The two stacked structural isomers have a form that can be described by an H, and are designated as H_1 and H_2 (Figure 4). The main feature of these conformations is coaxial helix-helix stacking by neighbouring helical stems, where the strands that pass between the quasi-continuous helices do not cross. This essentially is the conformation that we deduced from gel electrophoretic (16) and fluorescent energy transfer data (17). H_1 is constructed by stacking stem B on stem H, and stem R

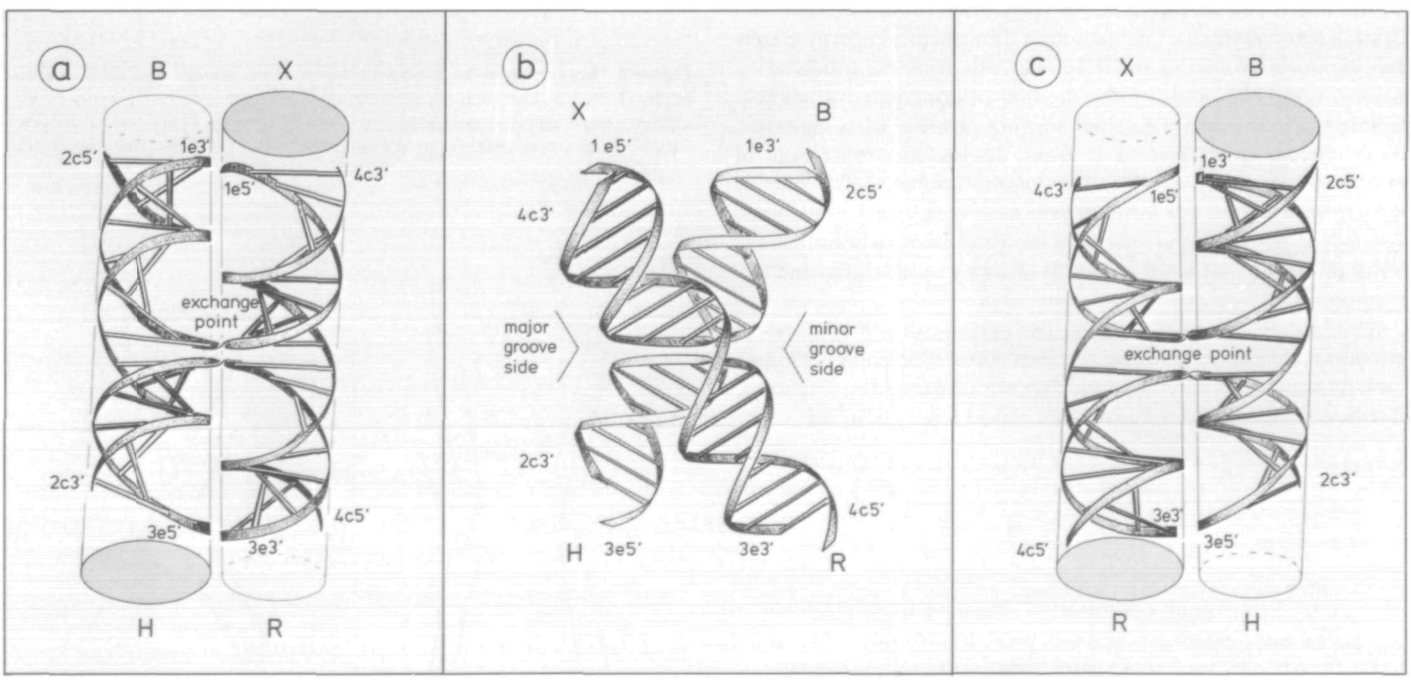

Figure 5 Simplified ribbon models of the right-handed, antiparallel DNA four-way junction structure H_1. Several terms used in the text are introduced. The structure consists of four stems X, B, H and R. Pairs of stems are stacked B on H and R on X (counting from the 5′-end of the continuous strands). The base pair step parameters at the junction of the stacked stems deviate only slightly from typical B-DNA parameters (see text). The outside of the sugar phosphate backbone is dotted and the sides of the bases directed towards the minor groove are darkened. Two of the four strands are continuous, in the sense that they follow a B-DNA like conformation even at the junction (strands 2 and 4). These are identified by 2c or 4c, followed 5′ or 3′ to indicate the polarity of the strand. The remaining two strands connect the two stacks at the exchange point, and exchange from one helix to the other (indicated by 1e or 3e). In a the major grooves of the two base pair steps at the junction point towards the viewer. b displays the face view of the same structure. Because the major grooves of the two base pairs steps at the junction are pointing into the same direction, we can identify a major and a minor groove side of the junction. In c the minor groove side points towards the viewer.

on stem *X*. H_2 is derived by an exchange of stacking partners such that stems *X* and *B* are coaxial, as are stems *H* and *R*. The structural properties of the junction between the two stems deviate only slightly from standard B-DNA with respect to base stacking (see below).

The third structure *E* may be described as a cross having an approximately square planar configuration. It is closely related to the starting structure with four *extended* arms. No mutual helix-helix stacking exists in this structure. This structure is closely related to that proposed to occur in the absence of specific metal ion binding (16).

Global conformation

A simplified view of an *H*-form four-way junction is presented in Figure 4. The four stems *X*, *B*, *R* and *H* (this notation follows that of junction 1 in Duckett *et al* (16)) are made by the strands (4,1), (1,2), (2,3) and (3,4), respectively. In the structure of H_1, stem *B* stacks on stem *H* while stem *R* stacks on stem *X*. Strand 2 starts in stem *B* and proceeds continuously to stem *H* without the helical symmetry being significantly disrupted at any point; strands of this type will be termed continuous strands. Stack *BH* is connected to stack *RX* via the exchanging strands 1 and 3. Exchanging strand 1 starts in stem *X* and ends in stem *B*, while exchanging strand 3 starts in stem *H* and ends in stem *R*. The minor grooves of stem *X* and stem *H* are accommodated in the major grooves of stems *B* and *R*, respectively (Figure 5). This avoids a steric clash of the strands at the junction. Steric hindrance is further reduced because the axes of *BH* and *RX* are not parallel. In Figure 5b, in which the molecule of Figure 5a has been rotated by −90°, stack *RX* lies on top of stack *BH*. The axes of these two helices subtend an angle of 50°to 70°.

The continuous strands 2 and 4 pass through the major groove of stem *R* and stem *B*, respectively. Because the two major grooves of the junctional base-pair steps of the two helices point in the same direction (to the left, in the case shown in Figure 5b), this side is designated the major groove side. Correspondingly, the two minor grooves point into the opposite direction which is called the minor groove side (to the right, in Figure 5b).

The geometry of the H_2 structure is similar to that of structure H_1, however, the stems stack in the opposite way. In H_2, stem *X* stacks on stem *B* and stem *H* on stem *R*. Since the DNA sequences of the four stems are different, the manner of the base stacking around the junction is different, and structures H_1 and H_2 are not equivalent. The stacking pattern of H_1 is given by:

```
|   |   |   |
C · G – A · T
|               |
C · G – A · T
|   |   |   |
```

whereas that of H_2 is given by:

```
|   |   |   |
A · T – T · A
|               |
G · C – C · G
|   |   |   |
```

In the case of the structure H_1 the purines are situated on the exchanging strands, generating a turn of the sugar phosphate backbone at the junction, while in H_2 they are located on the continuous strands.

The structures H_1 and H_2 are right-handed, antiparallel crosses. As shown in Figure 5b, the coaxial helical stack of stem *R* on *X* is rotated in a right-handed sense with respect to the stack of stem *B* on *H* below. The term 'antiparallel' indicates that the exchanging strands enter and leave the junction in nearly the opposite directions while the continuous strands run antiparallel (neglecting the open angle of the cross). These properties have both been demonstrated experimentally (16,17).

Figure 6 shows a ribbon model of the *E* structure. The base pairs at the junction display their major grooves towards the viewer. The structure is close to square planar. The four arms are unstacked and maximally extended. Colour pictures of the optimised H_1 structure are given in Figure 7.

To determine the orientation of the four helical DNA stems to one another, a best plane has been calculated from the four stem axes (see Theoretical Methods). The angles of the stem axes z_B, z_H, z_R and z_X to the average z-axis projected into the best planes (ψ_B, ψ_H, ψ_R and ψ_X, respectively) are given in Table 1 for H_1, H_2, and *E*, respectively. The acute angles between two arms vary between 43°and 67°. They are smaller in H_1 compared to H_2. The angles between the stems of the *E* structure are between 80°and 114°.

The deviations of the stem axes from the best plane (ϕ_B, ϕ_H, ϕ_R, ϕ_X) are also presented in Table 1. The bends of the stems at the junction in the H_1 structure are 15° for stem *X* stacking on *B* and 5° for stem *H* stacking on *R*. These angles are of the same order as bends induced in short DNA molecules in crystal lattices (for a review see Shakked (31) and cited literature). The values of the angles for the extended *E* structure (see Table 1) indicate that this structure is not perfectly planar but the stem axes are oriented to one side. This may be expected from the symmetry of the extended form *E* since the minor grooves of the base pairs at the junction are all facing towards the same side

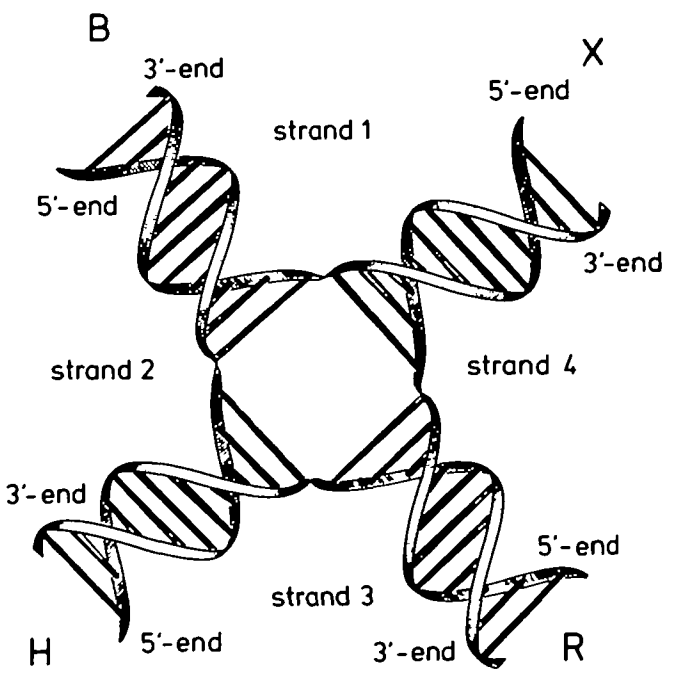

Figure 6. A ribbon model for the extended structure *E*. In each case the major groove of the base pair at the junction is pointing towards the viewer.

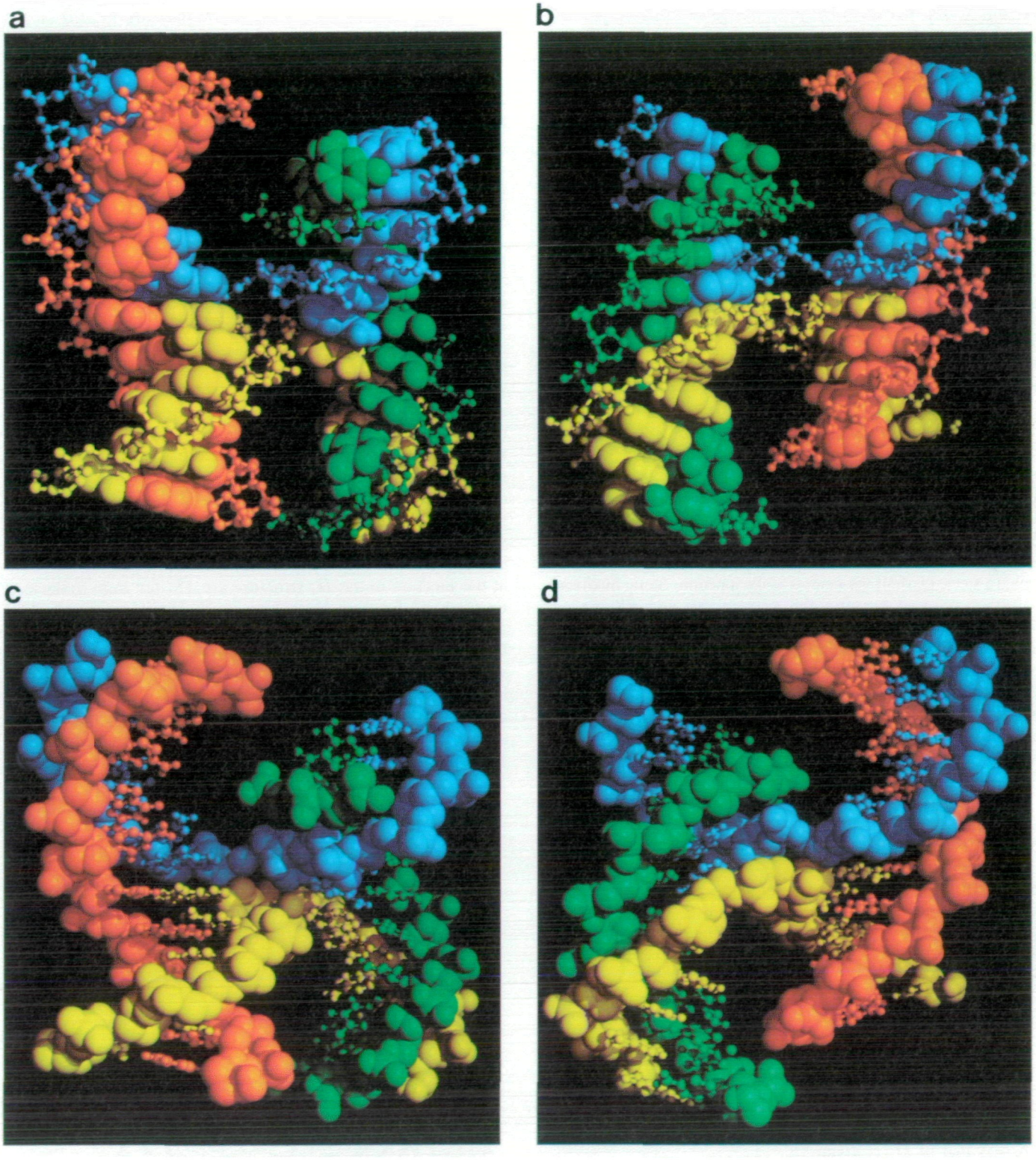

Figure 7. Computer-drawn illustrations of the optimised structure H_1. The strands are colour coded: blue for strand 1, red for strand 2, yellow for strand 3 and green for strand 4. a and b show major and minor groove views respectively, the backbone is drawn by stick and ball and the base atoms enlarged. This clearly shows the stacking of the stems c and d present the major and minor groove views respectively, where the backbone atoms are enlarged, with stick and ball representation of the base atoms

(see Figure 5). Gel migration experiments in the absence of divalent ions are consistent with this observation. We observed that the four slowly migrating species (each being cleaved in two different arms) have electrophoretic mobilities that are not exactly identical (16), consistent with a slight deviation from exact planarity of the arms.

The local structure at the junction

In order to estimate the continuity of the helical structure in H_1

Table 1.

Structure	ψ_B	ψ_H	ψ_R	ψ_X	ϕ_B	ϕ_H	ϕ_R	ϕ_X
H_1	28 3	−161 5	156 3	−22 4	−6.3	−8 9	5.8	2.2
H_2	145 0	−150 1	35.3	−32.6	−10.0	2 2	3 0	−10 7
E	−131.6	143.7	29.6	−49 5	−0.7	21.5	14.1	11.2

The orientation of the stem axes. The angles of the four stem axes for all three structures are given as shown in Figure 3. ψ_N gives the angle of the helix axis of stem N with the average of all four stems axes projected on the best plane spanned by the four helix axes (N being B, H, R and X). ϕ_N is the deviation of the helix axis of stem N from the best plane.

Table 2.

a Structure H_1

	stack	wedge	roll	tilt	twist	slide	shift	rise
H_1	*XB*	134 9°	−6 3°	171.4°	44.8°	−0.3°	−5.1 Å	17.8 Å
	HR	150 1°	−4 7°	169.3°	28.4°	−0 6°	−4.5 Å	18.1 Å
	BH	18.3°	−18 9°	−1.6°	29.7°	−1.6°	−1 4 Å	2.8 Å
	RX	3 6°	−3 4°	−1.5°	28.1°	−1.8°	−0.7 Å	3.4 Å

b Structure H_2

	stack	wedge	roll	tilt	twist	slide	shift	rise
H_2	*XB*	2.2°	1 6°	−1.6°	28 6°	−1 6°	−0.8 Å	3.9 Å
	HR	12 7°	13.1°	−2.3°	33 1°	−0.5°	−0 5 Å	4 3 Å
	BH	125 5°	−61 2°	−117 7°	53.7°	−2.0°	−4 1 Å	14 6 Å
	RX	120.7°	68 4°	103.3°	−51.4°	1 4°	−8.7 Å	−12.7 Å

c Structure E

	stack	wedge	roll	tilt	twist	slide	shift	rise
E	*XB*	83 5°	−27 1°	−78 5°	18 3°	0 7°	−4.7 Å	13.0 Å
	HR	85.3°	1 4°	−88.3°	26 8°	0 8°	−2 8 Å	13.7 Å
	BH	101.4°	−32.6°	−95 1°	22.6°	1 0°	−2 5 Å	14 2 Å
	RX	106 4°	−44 4°	−102.4°	44.8°	−0.7°	−4.3 Å	13.2 Å

The helical parameters of the junctions. The helical parameters of the junction are calculated according to the definitions agreed in an EMBO workshop in Cambridge (30) The helical parameters of stack *XB* means that the parameters are calculated stepping from the base pair of stem X to the junctional base pair of stem B (i e for the base pair stem A_6 T_{43} to G_7 . C_{18}).

Table 3.

strand number	stem	end	base	width (Å)	base	end	stem	strand number
2	*B*	5′	G_{13}					
			C_{14}					
			G_{15}					
			C_{16}	6.2	C_{12}	3′	*B*	1
			G_{17}	9 1	G_{11}			
2	*B*		C_{18}	8.4	C_{10}			
2	*H*		C_{19}	6.3	G_9			
			G_{20}	7 2	C_8			
			C_{21}	10 2	G_7	5′	*B*	1
			G_{22}	8.3	G_{30}	3′	*H*	3
			C_{23}	8.1	C_{29}			
2	*H*	3′	G_{24}	9.1	G_{28}			
					C_{27}			
					G_{26}			
					C_{25}	5′	*H*	3

The minor groove width of stem B on stem H in structure H_1 The minor groove width is measured by the distance of adjacent $C_{4'}$ atoms. The first and last column contain the number of the participating strand (see Figure 1). The indices of the stems are given under 'stem' and the polarity of the strands under 'end' The names and numbering of the bases are found under 'base'.

in passing from stem *B* to stem *H* and from stem *R* to stem *X* (the stacking stems, respectively), the helical parameters of the junction base pairs were calculated according to the Cambridge definitions (30). All the helical parameters are given in Table 2a for structure H_1. A corresponding calculation was performed for structure H_2 (Table 2b). In these tables the relative orientation of the junction base pair (i.e. the base pair located immediately at the four-way junction) of a given stem is given relative to the junction base pairs in the two neighbouring stems (i.e. those having common strands). The local tilt angles for the base pair steps between stem *X* and stem *B*, and stems *H* and *R* are of the order of 170° indicating that these stems are fully unstacked. By contrast, the steps from stems *B* to *H* and stems *R* to *X* display fairly normal helical parameters for B-DNA. The roll angle of stem *B* to *H* (−18.9°) is slightly smaller than in standard B-DNA. These steps are underwound having a twist angle of ~30°. A similar situation is found for structure H_2; here the values of the helical parameters indicate that stem *X* stacks on stem *B*, and stem *H* stacks on stem *R*, with only minor deviations from average B-DNA helical parameters. Again, the helical twist at the junction is underwound.

The exchanging strand invades the other helix close to where the second exchanging strand leaves that helix. To permit this strand exchange while avoiding close contacts of the backbones, the minor grooves of the two helices must open. The minor groove width is measured by the closest distance between the $C_{4'}-C_{4'}$ atoms across the minor groove of the stack *BH* of structure H_1. The values obtained are presented in Table 3. The minor groove width of the stack *RX* in the H_1 structure and the two stacks in structure H_2 show the same behaviour (data not shown). Small sequence dependent variations in the minor groove width values were expected and found. Starting from the 5'-end of the continuous strand of stem *B*, the minor groove opens as the junction is approached (see Table 3), and narrows again directly after the junction. This effect is illustrated in Figure 8.

Further examination of the helical parameters of the H_1 structure (Table 2) shows that there is a rather small twist angle between the base pairs at the junction going from one stem to the next stacking stem. These low helical twist angles of the two base pair steps at the junction in the two helices might be a consequence of the opening of the minor groove due to strand exchange.

For the approximately planar *E* structure the situation is strikingly different. The local tilt angles for the base pair steps at the junction are close to 90°. Thus, in the unfolded *E* structure the central base pairs do not stack. In the absence of Mg^{2+} ions these junctions exhibited a reactivity with osmium tetroxide, indicating that the base pairs at the junction are indeed not stacked (16). Most local roll angles are negative, indicating that the *E* structure is a very shallow pyramid with the four major grooves at the top.

The backbone angles

The backbone angles are given in Table 4a and b for H_1 and *E*, respectively, according to the IUPAC-IUB (32) recommendations. The angles not involved in the junctions adopt standard backbone angles (i.e. falling into expected ranges of g^+, t or g^-) found in the crystal structures of B-DNA oligonucleotides (31). An exception is the $g^- g^-$ motif for $\beta\ \gamma$ for the guanine in alternating GC.

The backbone angles of the bases building the junction in the exchanging or the continuous strands scatter considerably. The only angle that is in the same range for all turns is $\epsilon \sim g^-$ (the angle around $C_{3'}-O_{3'}$). The turn in H_1 between the bases G_{30} A_{31} and the turn in H_2 between the bases T_{42} T_{43} indicates that a major adjustment in ϵ is sufficient to create the overall turn. This angular rotation changes the orientation of the phosphate group, from partly pointing into the major groove to pointing into the minor groove (see Figure 9). This reorientation of the phosphate groups greatly reduces the electrostatic repulsion between the phosphate groups of the exchanging strands at the turn, which otherwise would come very close to one another. The same motif for ϵ is also found for all four junction backbone ϵ's for the extended planar structure *E* as given in Table 4b.

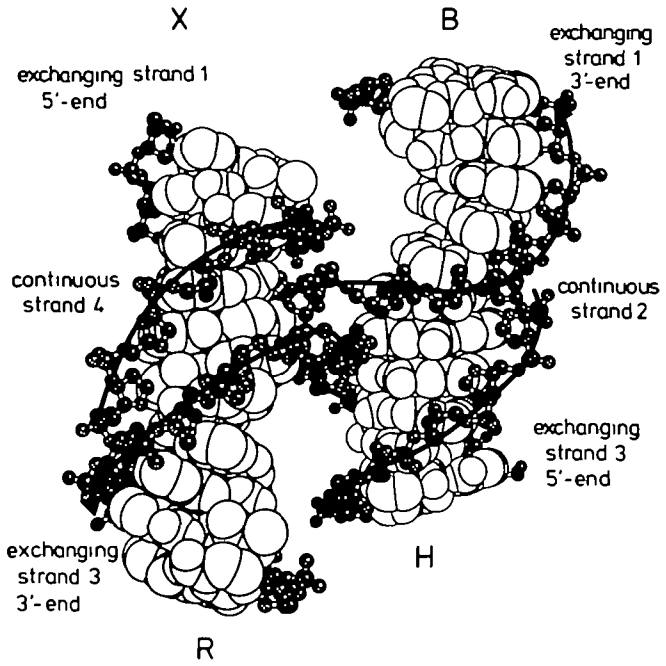

Figure 8. The minor groove side of the model of H_1. To avoid a steric clash between the two exchanging sugar-phosphate backbones, the minor groove must open at the junction. Starting at the 5'-end of the continuous strand, the minor grooves open at the junction and close immediately behind it.

Energies

The structural energies of the three structures H_1, H_2, and *E* are different (see Table 5). H_1 is the structure with the lowest energy. This structure was found experimentally for a junction closely related in sequence to that studied here (17).

Coordination of divalent ions

The formation of a stacked conformation requires the presence of counter ions (divalent or higher charged ions, 16, 33). We may therefore consider possible locations where counter-ions may bind to phosphate groups of different strands. Since the phosphate groups at the turn itself are pointing in different directions (see Figure 9), it is unlikely that they are able to coordinate the same divalent counter ion. Indeed, when phosphates were replaced at the junction in the continuous strands by electrically neutral methyl phosphonates (33), the junction isomerised such as to place the neutral phosphate analogues at the exchange point, the previously continuous strands now becoming the exchanging strands. Our interpretation of this observation is that the electrostatic repulsion of these phosphates at the exchange point are not compensated by ionic binding of particular (divalent) ions. As a consequence, an electrostatic repulsion will remain at the

Table 4.

a Structure H_1

		α	β	γ	δ	ε	ζ	χ + 180
1	A	−53 5	162.6	72 5	109.3	172.5	−104 2	39.3
	G	−61 9	−178.6	61.4	144.4	−179 9	−93 9	54 3
*	A	*−70 4*	*−174.4*	*57 4*	*137 7*	**−71.0**	*−103 0*	*62.4*
*	G	*64 1*	*−175.0*	*−62.1*	*158 5*	*−179 2*	*−89 7*	*38 8*
	C	−77 1	−165 2	56 8	148 3	−171 0	−66 7	57 0
	G	−55 5	−80.2	−63 6	163 4	174 9	−88 6	64.2
2	C	−72 9	178.5	58 6	144 4	−169 7	−66 0	68.8
	G	−49 0	−74.3	−77 5	167 3	174 5	−107 9	67.5
¦	C	*59.0*	*170.4*	*−72 9*	*167 4*	*−75 4*	*160 0*	*69.0*
¦	C	*−86.2*	*142.8*	*44 4*	*141 7*	*−170 0*	*−66 2*	*60.5*
	G	−55.0	−79.0	−67 5	163 3	170 1	−92 6	69.4
	C	−67.4	177.8	62 4	149 9	−173 3	−65 4	71.0
3	G	−53 2	−77.4	−69.7	163 2	171 7	−89 2	70 2
	C	−71 0	−179 2	60 0	140 4	176 6	−93 2	69.7
*	G	*−72.8*	*−172 7*	*50 8*	*132 7*	**−61.5**	*−61.4*	*66.2*
*	A	*−68 8*	*−163.3*	*56.2*	*120 6*	*−169 4*	*−95 9*	*25 2*
	G	−81 8	−172 7	57.1	140 6	173 5	−96 1	64.6
	A	−61 6	−176 5	63.4	125 5	−173 8	−143 5	69 8
4	T	−59 8	174 8	65 5	146 8	−162 1	−170 8	61 1
	C	−49 6	135 8	63 4	134 3	−171 5	−87 0	43.4
¦	T	*−74 0*	*−176.9*	*54.7*	*114 5*	*176 2*	*−92 4*	*44.1*
¦	T	*−67 9*	*179 2*	*57 8*	*126 2*	*174 9*	*−104 6*	*62 3*
	C	−66 2	177 4	59.7	139 4	176 1	−102 5	61.2
	T	−65 9	−176 1	60 9	145 5	−170 4	−148 1	58 5

b Structure E

		α	β	γ	δ	ε	ζ	χ+180
1	A	−60 2	163 7	68 3	144 2	172 7	−107 2	58 7
	G	−62 3	−177 6	62 3	143.6	179 4	−95 9	51 4
*	A	*−74 0*	*−170 6*	*54 1*	*133 7*	**−74.1**	*−177 1*	*59 5*
*	G	*57 5*	*176.4*	*−73 2*	*155 6*	*169 7*	*−101 1*	*73 3*
	C	−67 8	−179 5	63 1	150 7	−173 1	−65 2	66 3
	G	−52 6	−75 8	−71 3	163 3	168 8	−90 2	70 6
2	C	−70 8	−179 1	61 1	148 0	−172 6	−65 4	69 5
	G	−57 8	−81 3	−68 5	163 7	177 8	−118 7	68 7
*	C	*57 4*	*168 0*	*−61 3*	*169.5*	**−81.1**	*157 0*	*90 1*
*	C	*47 6*	*94 6*	*44 6*	*126 0*	*−171 1*	*−67 4*	*53 7*
	G	−50 3	−74 1	−72 1	162 6	165 8	−92 6	76 3
	C	−66 7	179 9	62 6	148 9	−173.0	−66 0	66 7
3	G	−52 3	−76 5	−70 6	163 1	169.3	−91 9	68 5
	C	−68 1	−179.7	62 2	149 2	−172 0	−64 1	66 7
*	G	*−63 4*	*−92 3*	*−63 7*	*166.0*	**−72.1**	*−155 3*	*80 8*
*	A	*−68.2*	*178.5*	*58 3*	*150 2*	*−178 1*	*−119 2*	*85.1*
	G	−66 1	168.4	62 2	151 3	176 3	−114 7	74 9
	A	−66 3	−177 5	60 6	149 3	179 4	−116 8	75 1
4	T	−56 4	175 7	65 4	144 8	−170 4	−143 0	56 1
	C	−59 9	162 2	61 5	143 8	176 9	−100 6	54 5
*	T	*−67.4*	*−174 2*	*58.9*	*146 2*	*−69.2*	*−179 7*	*61 3*
*	T	*−59 8*	*179 0*	*62.0*	*141 2*	*175.5*	*−108 1*	*68 1*
	C	−63 4	176 0	60.6	142 4	171.1	−107 8	66 5
	T	−59 4	−179.3	61.2	138.7	−178.8	−109 1	53 6

The conformational angles of the backbones around the junctions in structures H_1 and E. Only the angles of the sugar-phosphate backbone close to the junction are shown. The first column contains the strand number (see Figure 1). An asterisk (*) indicates a turn in the strand (the junction of the exchanging strands in case of H_1 and in all strands for structure E). A vertical bar (¦) indicates the junctions of the continuous strands for the structure H_1. The bases at the junction from one stack to the other are indicated by bold face characters. Most angles at the junction are given in italics, the bold face ε-angle of the bases in the exchanging strand on the 5'-side of the junction is discussed in the text. The definitions of the angles are according to the proposals of the IUPAC-IUB Joint Commission on Biochemical Nomenclature (32).

exchange point of the structure. This repulsion (and thus the structural energy) can be strongly reduced by placing the uncharged phosphonates at this position.

Phosphate groups other than those at the turn might complex counter-ions. In the structure H_1 the 5'-phosphates of G_5 and A_6 come close to those of G_{28} and C_{29}, respectively. Both

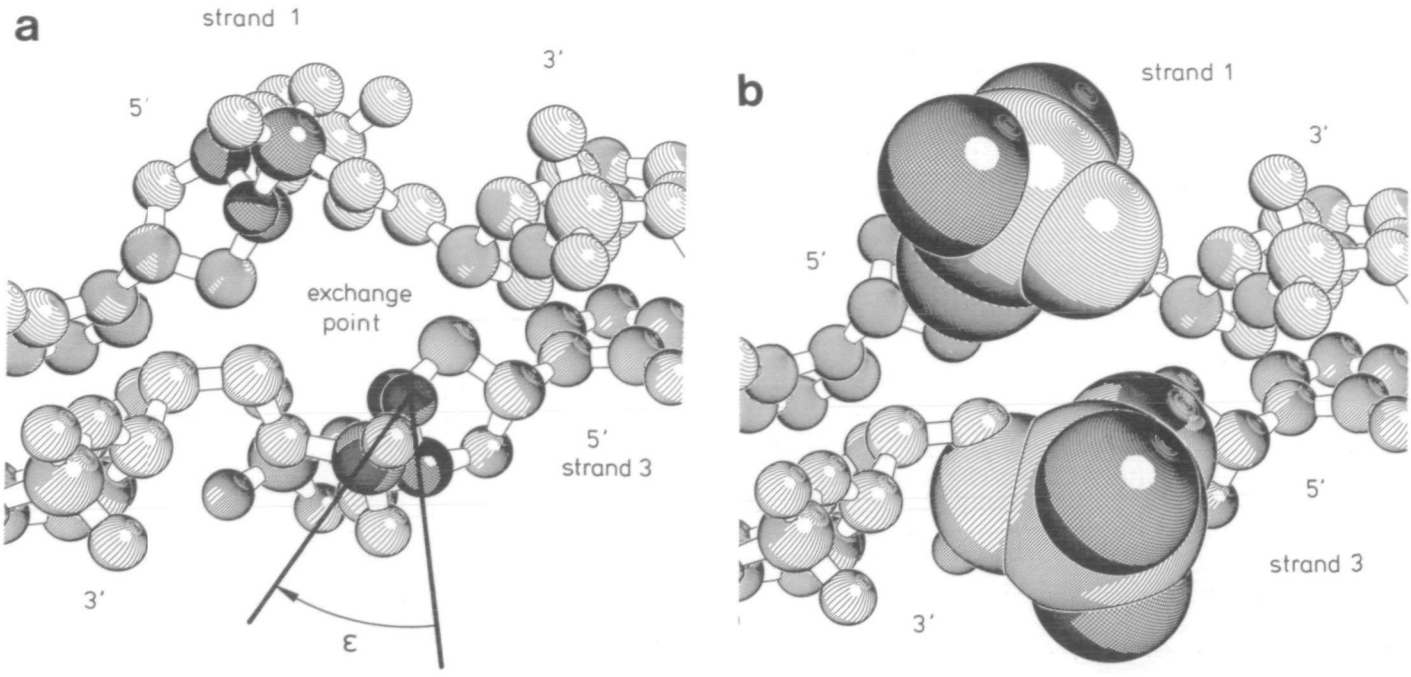

Figure 9. The backbone of the bases that generate the exchange point of the junction To avoid steric clash between the phosphates of the exchanging strands at the exchange point, the ϵ angle around $C_{3'}-O_{3'}$ adopts the g^- conformation, in contrast to the usual t conformation Strand 1 is displayed with latitudes and strand 3 with meridians In **a** only the atoms defining the ϵ angle have a crossed grid on both strands In **b** the radii of the atoms of the phosphate group are enlarged to their van-der-Waals values The anionic oxygen atoms are drawn with a crossed grid The orientation of these two phosphate groups probably prevents coordination of a shared cation

Table 5.

	E_{tot} $\times 10^3$	E_{bon} $\times 10^1$	E_{ang} $\times 10^2$	E_{dih} $\times 10^2$	E_{vdW} $\times 10^2$	E_{ele} $\times 10^2$	E_{HB} $\times 10^1$
H_1	−2 406	1 142	2 792	6 093	−8 766	5 947	−3 357
H_2	−2 391	1 198	2 776	6 281	−8 765	5 857	−3 360
E	−2 366	1.224	2 691	6 222	−8 254	5 749	−3.474

The internal energies (kcal mol^{-1}) of the three structures discused E_{tot} is the total energy, E_{bon} the bonding energy, E_{ang} the bond angle energy, E_{dih} the dihedral angle energy, E_{vdW} the van-der-Waals energy, E_{ele} electrostatic energy and E_{HB} the hydrogen bonding energy (23)

potential coordination sites are on the major groove side of the junction (see Figure 5b). In structure H_2 the 5'-phosphates of C_{18} and G_{20} come close to those of T_{42} and C_{44}, respectively. In this case the first site is on the major groove side, the second on the minor groove side.

DISCUSSION

A structure for the four-way DNA junction can be constructed by molecular mechanical modelling

We have shown that a model of the four-way junction in DNA can be successfully constructed, using a version of the AMBER program package that had been modified to include the effect of counterions and to allow for global optimisation. Stacking energies, hydration and electrostatic interactions are assumed to determine local structural variation in helical DNA, and we find that these factors also determine the structure of four-way junctions. We have identified three distinct structures using this approach. One contains four unstacked, extended helical arms in a square-planar configuration (the *E* structure), while the remaining two are isomeric arrangements in which pairs of helices associate via basepair stacking to form coaxial, quasi-continuous helices (the *H* structures). In the latter structures the colinear pairs of stacked helices are rotated in a right-handed sense, to subtend an angle of close to 60°, and the exchanging strands are disposed about this small angle, generating an approximately antiparallel geometry.

The global features of the theoretical model are closely similar to those of the structures found experimentally

The Holliday intermediate postulated for homologous genetic recombination is most frequently drawn as a parallel structure in textbooks, and in the model constructed by Sigal and Alberts (19) the helices were aligned side-by-side, with crossed exchanging strands. Such an arrangement is improbable due to large entropic terms; the resulting electrostatic repulsion would require extensive screening. McGavin (34) presented theoretical models of a four-way junction, which are similar to our extended *E* structure. This suggestion is not in agreement with the available experimental data for the structure in the presence of magnesium

and other ions (16,17). Calascibetta *et al* (35) presented a structural model for a four-way junction comprising two base-pairs in each stem, that included some aspects of the structure presented here. Their structure contained pairs of stems stacked in a B-DNA like conformation, and included the $\epsilon \sim g^-$ motif at the base at the turn on the 5′-side of the junction. Furthermore, the orientation of the axes of their stacked helices was antiparallel. However, in their structure the helices were not inclined at a mutual angle, and extending the stems in their structure to longer arms would result in unfavourable steric interactions.

The structures identified in this study are in excellent agreement with all experimental data. The extended ***E*** structure is closely similar to that proposed by us for the junction in the absence of bound metal ions. The unstacked structure would generate the pattern of four slow and two fast species seen by gel electrophoresis (16,33), and is consistent with the reactivity of thymine bases located at the junction (16).

In the presence of metal ions such as magnesium the junction is observed experimentally to undergo a marked structural reorganisation (16,33), and the ***H*** structures identified theoretically in this study are fully consistent with these and all other experimental data. First, the X-shape explains the observed relative gel mobilities of junctions with two long and two short arms. Experimentally we have observed that the six such possible species exhibit one of three possible migration rates, consistent with the long arms being colinear (fastest), or related by the ~60° angle (slowest) or the ~120° angle (intermediate mobility)—the 2:2:2 pattern. These conclusions were strengthened by fluorescence resonance energy transfer measurements on junctions having fluorescent dyes conjugated to the 5′ ends of different arms (17), thereby allowing estimation of the relative end-to-end distance for the six possible arm-arm distances in the junction. The results were in complete agreement with the deductions from the gel electrophoresis experiments, confirming the antiparallel stacked X-structure. Recent neutron scattering measurements of the radius of gyration of a junction containing two long and two short arms are also interpretable only in terms of an antiparallel structure (AIH Murchie, J Torbet and DMJL, unpublished data). The ***H*** structures are two-fold symmetric; Churchill *et al* (18) probed a synthetic junction using hydroxyl radicals, from which they concluded that the junction has two-fold symmetry.

Further confirmation of this model may be taken from the recent gel electrophoresis and transient electric birefringence data of Cooper and Hagerman (36). They studied a junction of different sequence from this work, and obtained a gel pattern closely similar to the 2:2:2 pattern. This can be interpreted in the same way that we have rationalised the gel data of our junctions. From the electric birefringence they deduced two small and four large angles, and the small angles are just those that we would have predicted from their gel data, based on the antiparallel ***H*** structures.

The model building, and basic stereochemical considerations, suggest that the stacked X-structure will be right-handed, in order to minimise steric overlap and increase mobility by locating the continuous strands to the 3′ side of the exchange point in the major groove of the opposing helix. The handedness has been confirmed experimentally by fluorescence energy transfer experiments (17). Moreover, we have recently shown that the 3′ side of the continuous strand is protected against cleavage by DNase I, at just the point where it should lie in the groove of the other helix (AIH Murchie, WA Carter, J Portugal and DMJL, unpublished data). Recently a crystal structure of a double-stranded dodecamer has been determined in which pairs of helices stack on top of each other at a mutual angle of 60°(37). The backbones of each helix are buried in the major groove of the other, thereby avoiding close contacts. This shows clear similarities with the model for the four-way junction; with the major difference that strand exchange occurs in the junction.

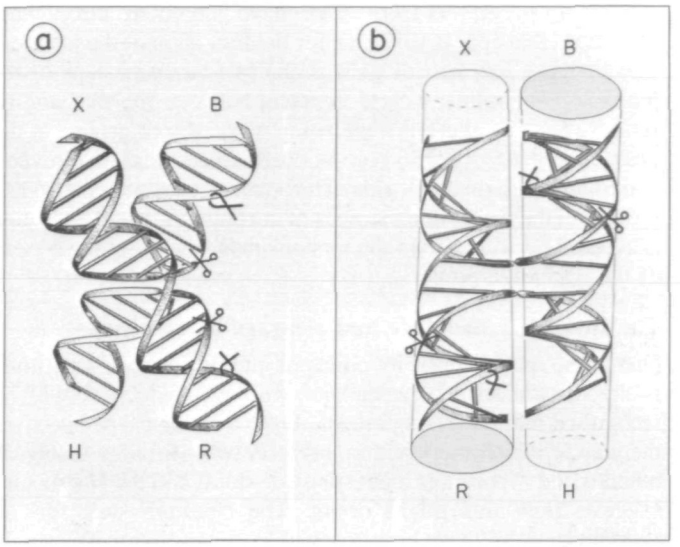

Figure 10. Cleavage sites for Holliday resolvase enzymes shown on the optimised structure H_1. T4 endonuclease VII cleaves four-way junctions on the exchanging strands 2 or 3 bases to the 3′ side of the point of strand exchange (16,20,38). These sites are indicated by the scissors symbols. Yeast resolvase cleaves cruciform structures about six bases from the exchange point, on the opposite strands from T4 endonuclease VII (39), these cleavage points are indicated by tongs symbols. Both sets of cleavages are shown on **a**, the face of the junction, and **b**, the minor groove side. Note that the sites for both enzymes are located on the minor groove side of the junction, suggesting that the enzymes interact with this side of the molecule.

Model building also suggests that the small angle of the ***H*** structure should be of the order of 60°. This is also in good accord with the available experimental data. From fluorescence energy transfer we were able to estimate the end-to-end distance across the small angles, from which the angle was calculated to be approximately 60° (17), while Cooper and Hagerman (36) were able to estimate one of their small angles as 58° by electric birefringence. From radius of gyration measurements we obtained a further estimate of the angle as 67° ± 20° (AIH Murchie, J Torbet and DMJL, unpublished data). While none of these data have the precision that would allow rigorous testing of the model, clearly all are fully consistent with the proposed model.

Our junctions were designed to have optimal stability, assuming that this would be increased by purine-purine stacking. As a result we obtained stable junctions where only one of the possible two isomers is significantly populated in the presence of magnesium. In the case of junctions having other sequences, the energy difference between the two high salt isomeric forms may be lower. This would result in a more even population of both isomeric forms.

Some local distortion of the DNA structure is required at the junction

In generating the H_1 and H_2 structures of the junction, coaxially stacked DNA helices were created with properties that are closely

similar to normal B-DNA. We have identified three main distortions that appear sufficient for the formation of the junction. The first is a low helical twist at the two basepair steps of the junction, that reduces close contacts between the exchanging strands. Second, there is a widening of the minor groove at the junction in the 5′ direction on the continuous strand, that reverts to normal width on the 3′ side. Third, contact between phosphate groups on the exchanging strands at the point of strand exchange is avoided by a change in the torsion angle $\epsilon \sim g^-$ at the 5′ side of the exchange point.

The two-sided structure and cleavage by resolvases

One of the most significant points of interest in the *H* structures is the dissimilarity between the two sides, which should be recognised differently by proteins. From a biological perspective, the way in which the junction interacts with Holliday resolvase remains one of the most interesting questions, and the *H* structure suggests how this might occur. The cleavage sites for T4 endonuclease VII have been mapped to the resolution of a single nucleotide both on synthetic junctions (16,20) and cruciform structures in supercoiled plasmids (38), and a consensus cleavage pattern emerges in which the resolvase cleaves the exchanging strands two or three bases from the exchange point on the 3′ side of the junction.

These cleavage sites are drawn on to the right-handed, non-crossed *H* structure in Figure 10. Both sites are located on the minor groove side of the junction, suggesting that the dimeric enzyme binds to this side of the molecule. Perhaps it is worth noting that if the junction were actually in the crossed, parallel conformation, the cleavage sites would lie on opposite sides of the molecule, which is hard to reconcile with the observed simultaneous cleavage. Another enzyme that resolves four-way junctions has been isolated from yeast (39). At first sight, comparison of the cleavages introduced into the same cruciform junctions by T4 endonuclease VII and the yeast enzyme appear to indicate that the two enzymes are very different—the yeast enzyme cleaves the opposite strand from T4 endonuclease VII, approximately three or four bases further from the junction. However, it can be seen from Figure 10 that these sites are located across the major groove from the T4 endonuclease VII sites, on the same face of the junction. Thus it seems that the enzymes probably bind in a very similar manner, but the active sites that accomplish the cleavage reaction are somewhat differently aligned in the two enzymes. The location of the bound resolvase enzyme is currently being investigated by footprinting and interference techniques.

Perspective

In summary, we have used molecular mechanical computer modelling techniques to generate a structure that is in remarkable agreement with all the available experimental data. While theoretical methods cannot in themselves prove a structure, they are valuable in a number of respects. First, this analysis has shown that the stacked X-structure, that was used to interpret gel electrophoretic data, is stereochemically sound. This is important, because the antiparallel structure was radically different from contemporary ideas of four-way junction structure, and has a number of potentially significant biological ramifications. These calculations show that there is no structural impediment that might make formation of the right-handed antiparallel structure impossible. Second, the model building exercise suggests stereochemical solutions to the problem of constructing the exchange point, where the strands pass between the different helices. Third, the theoretical analysis makes structural predictions that can be tested, and provides a valuable source of experimental ideas. The proposed sites of interaction with resolvase is one example of this; another is the potential ion binding sites identified in the structure. A further area in which a combination of theory and experiment may be productive lies in determining the rules that govern which stacking isomer will be more stable for any given sequence. At present it appears from the data that stacked purines are more stable on the exchanging strands, and it is encouraging that this is predicted correctly for junction 1 by the modelling However, a complete understanding of this is likely to require the analysis of many more sequences by a combination of theoretical and experimental methods.

These studies illustrate the value of combining theoretical and experimental approaches to the study of nucleic acid structure. We have generated a model for the structure of the four-way DNA junction that provides a framework for considering interactions with enzymes and other ligands. We are hopeful that this approach will continue to offer useful insight into this biologically important structure.

ACKNOWLEDGEMENTS

We thank Bob Clegg, Derek Duckett, Alastair Murchie and Tom Jovin for helpful discussions, and the Royal Society, and the Nuffield Foundation for financial support. We are grateful to H. Sebesse for his expert drawing of many of the figures. The Figures 7–9 were drawn by the SCHAKAL program written by E. Keller, University of Freiburg. We thank R. Klement for his help in using this program.

REFERENCES

1 Holliday, R (1964) *Genet Res* , 5, 282–304
2 Broker, T R and Lehman, I R (1971) *J Molec Biol* **60**, 131–149
3 Sobell, H M (1972) *Proc Natl Acad.Sci USA* **69**, 2483–2487
4 Sobell, H M (1974) In Mechanisms in recombination (Ed Grell, RF) Plenum, New York 433–438
5 Meselson, M S and Radding, C M. (1975) *Proc Natl Acad Sci USA* **72**, 358–361
6 Orr-Weaver, T L , Szostak, J W and Rothstein, R J (1981) *Proc Natl Acad Sci USA* **78**, 6354–6358
7 Hoess, R., Wierzbicki, A and Abremski, K. (1987) *Proc Natl Acad Sci USA* **84**, 6840–6844
8 Kitts, P A and Nash, H A (1987) *Nature* **329**, 346–348
9 Nunes-Düby, S E , Matsomoto, L and Landy, A (1987) *Cell* **50**, 779–788
10 Jayaram, M , Crain, K.L , Parsons, R L and Harshey, R M (1988) *Proc Natl Acad Sci USA* **85**, 7902–7906
11 Bell, L R. and Byers, B (1979) *Proc Natl. Acad. Sci USA* **76**, 3445–3449
12 Kallenbach, N.R , Ma, R -I and Seeman, N C. (1983) *Nature* **305**, 829–831
13. Gough, G W. and Lilley, D.M J (1985) *Nature* **313**, 154–156.
14 Diekmann, S and Lilley, D M J. (1987) *Nucl Acids Res* , **14**, 5765–5774
15. Cooper, J P and Hagermann, P.J (1987) *J Molec Biol.* **198**, 711–719
16. Duckett, D R , Murchie, A I.H , Diekmann, S , von Kitzing, E , Kemper, B and Lilley, D M J. (1988) *Cell* **55**, 79–89
17 Murchie, A I H , Clegg, R.M., von Kitzing, E., Duckett, D R , Diekmann, S and Lilley, D M.J (1989) *Nature* **341**, 763–766
18. Churchill, M E A., Tullius, T.D., Kallenbach, N.R and Seeman, N.C (1988) *Proc Natl Acad Sci. USA* **85**, 4653–4656
19 Sigal, N and Alberts, B (1972) *J. Molec. Biol* **71**, 789–793.
20. Mueller, J E , Kemper, B., Cunningham, R.P , Kallenbach, N.R. and Seeman, N C (1988) *Proc. Natl. Acad Sci USA* **85**, 9441–9445.
21 Weiner, P K. and Kollman, P. (1981) *J Comp. Chem.* **2**, 287–303
22 Rao, N S and Kollman, P (1985) *J. Am. Chem Soc.* **107**, 1611–1616
23 von Kitzing, E (1986) Molekülsimulation mit Hilfe von Kraftfeldrechnungen

am Beispiel der Aggregation von Nukleinsäuren verschiedener Konformation zu einem Komplex mit Übersetzungsfunktion, Edition herodot/Rader Verlag, Aachen 1986
24 von Kitzing, E and Diekmann, S (1988) *Eur.Biophys J*, **15**, 13–26.
25 Shanno, D.F (1978) *SIAM J Numer. Anal.* **15**, 1247–1252
26 Sklenar, H, Lavery, R and Pullman, B (1986) *J. Biomolec Struct Dyn* **3**, 967–987.
27 Bremermann, H. (1970) *Math Biosci* **9**, 1–15
28 Rao, G S, Tyagi, R.S and Mishra, R.K (1981) *Int J Quant. Chem* **20**, 273–279.
29 Rinnoy, Kan, A.H G, Boender, C.G.E and Timmer, G T H (1985) in Klaus Schittowsky, Computational Mathematical Programming, Springer Berlin, Heidelberg, New York, Tokyo
30 Dickerson, R E (1989) *EMBO J.* **8**, 1–4.
31 Shakked, Z and Rabinovich, D (1986) *Prog Biophys Molec Biol* **47**, 159–195
32 IUPAC-IUB Joint Commission on Biochemical Nomenclature (JCNB) In Pullman, B and Jortner, J (eds) Nucleic acids. the vectors of life, Reidel, Dortrecht, pp. 559–565
33 Duckett, D R, Murchie, A I H and Lilley, D.M J (1990) *EMBO J* **9**, 583–590
34 McGavin, S (1989) *J Theor Biol.* **138**, 117–128
35 Calascibetta, F G, De Santis, P, Morosetti, S, Palleschi, A and Savino, M (1984) *Gazz. Chim Ital*, **114**, 437–441
36 Cooper, J.P and Hagerman, P J (1989) *Proc Natl Acad. Sci USA* **86**, 7336–7340
37 Timsit, YU, Westhof, E, Fuchs, R P P and Moras, D (1989) *Nature* **341**, 459–462
38 Lilley, D M J. and Kemper, B (1984) *Cell* **36**, 413–422
39 West, S C, Parsons, C A and Picksley, S M (1987) *J Biol. Chem.* **262**, 12752–12758